JOURNAL OF MATERIALS SCIENCE 19 (1984) 2378–2386

Superplastic deformation of strongly textured Ti–6 Al–4 V

Part 1 *Stress and strain anisotropy*

D. S. McDARMAID, A. W. BOWEN, P. G. PARTRIDGE
Materials and Structures Department, Royal Aircraft Establishment, Farnborough, Hants, UK

Stress and strain anisotropy of a strongly textured Ti–6 Al–4 V alloy bar during superplastic deformation at 880 and 928° C has been investigated. After ~ 0.9 superplastic strain at 928° C the deformation tended to become isotropic. The anisotropic superplastic deformation was found to be dependent upon the aligned microstructure and not influenced by the original α-phase crystallographic texture. The room-temperature anisotropy before and after superplastic plastic deformation was controlled by the original α-phase texture, which was still present even after 1.48 strain (344% elongation) at 928° C.

1. Introduction

Superplastic forming is normally associated with uniform plastic deformation to large strains [1, 2] and isotropic deformation. Many investigations, however, have observed a stress anisotropy at superplastic deformation temperatures and several others a strain anisotropy. In the latter case, round cross-sections become elliptical after superplastic deformation of eutectic and eutectoid Zn–Al [3–5], eutectic Sn–Pb [6] and a copper-bronze alloy [7–9]. The origin of such anisotropy at elevated temperatures has been related to the original crystallographic texture and the operative slip systems in several Zn–Al alloys [3, 4, 10], and to the presence of an aligned microstructure in eutectic Sn–Pb [6] and an Al–6 Cu–0.5 Zr alloy [11]. In other investigations, however, it was not possible to isolate the effect of texture from the effect of aligned microstructure [7, 9, 12].

Room-temperature anisotropy in α/β titanium alloys is well deconumented [12–15] and is known to be related to crystallographic textures developed in the h c p α-phase during the manufacturing process, which dictates the resultant preferred deformation-modes [16]. At the superplastic forming temperature for Ti–6 Al–4 V, 900 to 950° C, the deformation process would be expected to be independent of room-temperature texture owing to an increased proportion of the more ductile β-phase and an increase in the available slip systems, with similar critical resolved shear-stresses in the α-phase. The α/β phase ratio changes from ~ 90/10 at room temperature to ~ 50/50 at the superplastic temperature. This is in agreement with the conclusion of Paton and Hamilton [17] that microstructural features rather than texture determine the ability of Ti–6 Al–4 V sheet to deform superplastically. However, increased strain anisotropy has been reported with increased test temperature over the temperature range − 196 to 700° C in textured commercial-purity titanium [18] tested at a strain rate of $2.7 \times 10^{-4}\,\text{sec}^{-1}$, which is similar to that used for superplastic deformation. In this case the anisotropy was attributed to a decrease in the amount of twinning with increased temperature since twinning produces more isotropic strain. Kaibyshev *et al.* [19] have also reported that for VT6 titanium alloy (Ti–6.5 Al–5.1 V) sheet the presence of a strong initial texture enables superplastic deformation to occur at lower temperatures and higher strain rates.

As crystallographic textures are always present in titanium alloys, the present investigation was

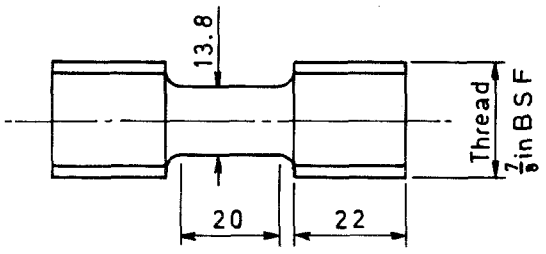

Figure 1 Test piece geometry.

undertaken to clarify the roles of α-phase texture and microstructure in the development of anisotropic deformation at elevated temperatures. A rectangular-section bar, which had a strong basal-edge texture parallel to the long transverse direction and a fine-grained aligned microstructure in the longitudinal (rolling) direction was selected for the present study. This enabled test pieces with the round cross-sections to be machined from the three principal directions of the bar. The present paper describes the stress and strain anisotropy observed. Details of the microstructural and textural changes will be described in Part 2 [20].

2. Material and test procedure

A rectangular bar, 160 mm x 55 mm, was supplied by IMI Titanium Ltd. The composition was 6.34 Al, 4.35 V, 0.18 Fe, $\leqslant 0.006$ H_2, < 0.01 N_2, 0.150_2, balance titanium. Prior to machining the bar was mill annealed for 4 h at 700° C and air cooled. Round test pieces (Fig. 1) were cut from the longitudinal (L), long transverse (LT) and short transverse (ST) directions; a reduced thread section and a 13.00 mm gauge diameter were necessary for the ST test pieces.

The elevated-temperature deformation was carried out at constant crosshead velocity on an Instron model TT-C tensile machine. The test temperature ($T \pm 2°$ C) was maintained over ~ 100 mm using a three-zone furnace. A deoxygenated argon atmosphere, with a slight back pressure, was maintained in a silica-glass environment chamber surrounding the pull rods and test piece. Three tests were interrupted after predetermined strains and the test piece cross-sections measured. The gauge lengths of these test pieces were then remachined and the process repeated.

3. Results

The effect of initial strain rate ($\dot{\epsilon}_I$) on the flow stress at 928° C for the three principal directions of the bar are shown in Fig. 2. Deformation at $\dot{\epsilon}_I = 4.2 \times 10^{-3}\,sec^{-1}$ and $1.05 \times 10^{-2}\,sec^{-1}$ was nonsuperplastic, i.e. the gauge-length necked owing to plastic instability. Superplastic deformation occurred at $\dot{\epsilon}_I = 4.2 \times 10^{-4}\,sec^{-1}$ and $1.05 \times 10^{-3}\,sec^{-1}$; the strain-rate sensitivity for these strain rates was 0.64 and 0.59, respectively. Under superplastic conditions the relative flow stresses were $\sigma_L > \sigma_{LT} > \sigma_{ST}$, whereas under nonsuperplastic conditions the flow stresses became similar with increasing strain rate. With increasing strain, and at all strain rates, the cross-sections of the test pieces became elliptical.

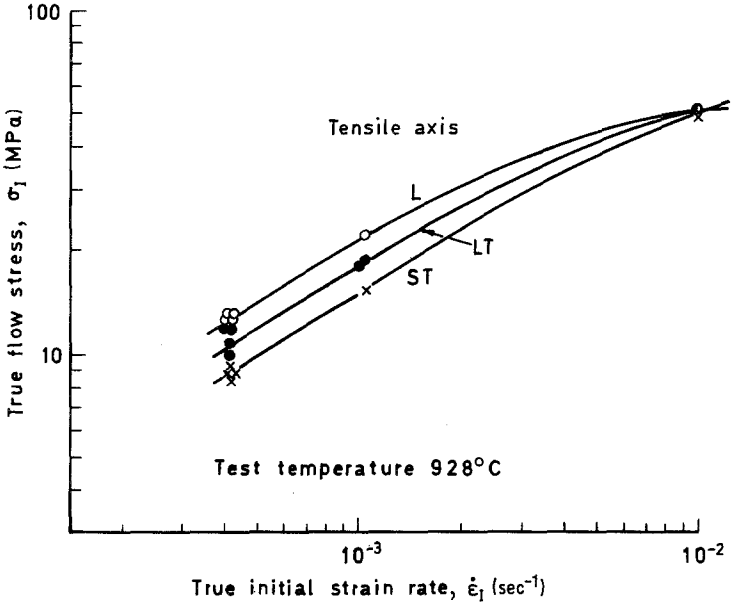

Figure 2 Effect of test direction on the log σ_I against log $\dot{\epsilon}_I$ curve at 928°C.

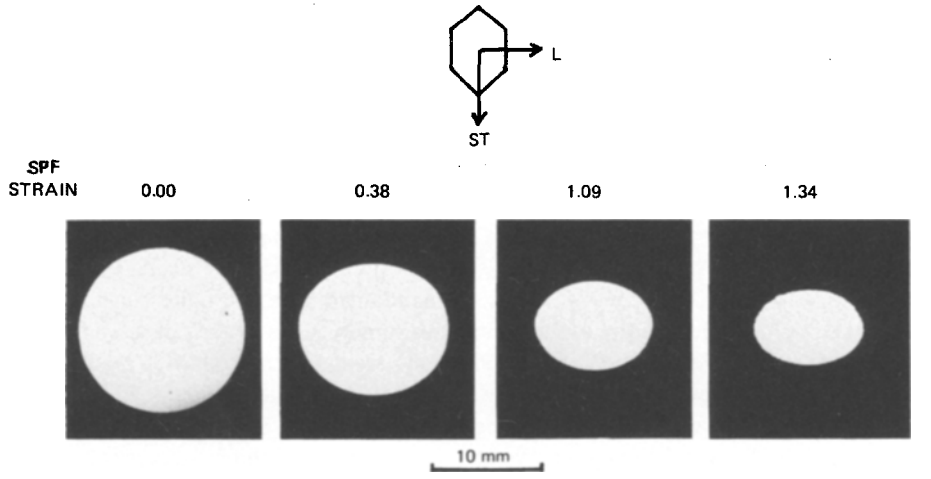

Figure 3 Anisotropic deformation with superplastic strain at 928°C and $\dot{\epsilon}_I = 4.2 \times 10^{-4}$ sec^{-1} in the LT direction.

Typical cross-sections as a function of superplastic strain for the LT test pieces are shown in Fig. 3. In this example, the diametral strain $\epsilon = \ln (d_0/d)$, where d_0 and d are the initial and final diameters, respectively, was greater in the ST direction than in the L direction, i.e. the strains were inversely proportional to the initial axial flow stress. This relationship between diametral strain and initial flow stress was found for all test pieces. The axial superplastic strain, $\ln (A_0/A)$, where A_0 and A are the initial and final cross-sectional areas, and the maximum and minimum diametral strains are plotted in Fig. 4. The data show that the respective diametral strains were dependent upon

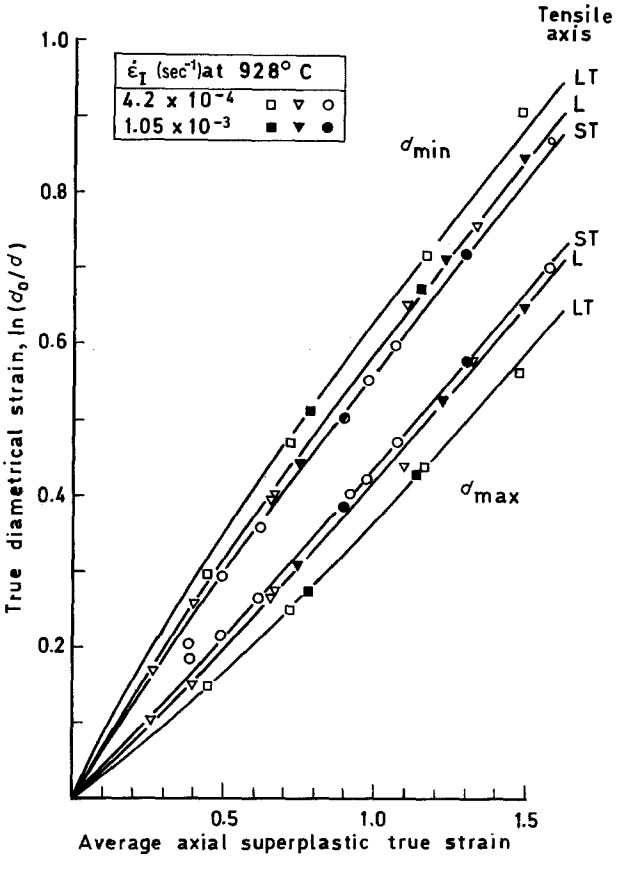

Figure 4 Effect of axial superplastic strain and strain rate at 928°C for the L, LT and ST directions of the bar on the maximum and minimum diametral strains.

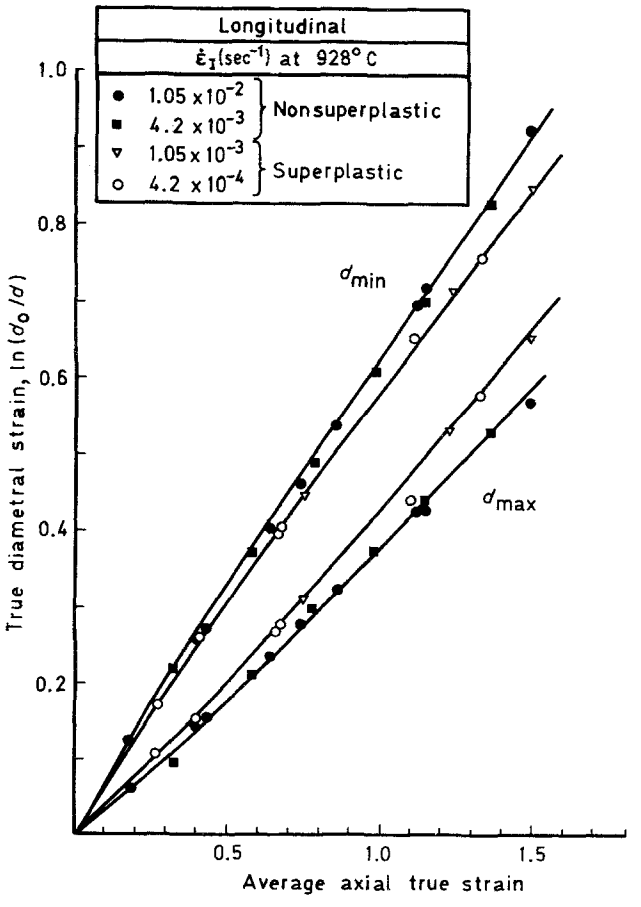

Figure 5 Effect of axial strain and strain rate on the maximum and minimum diametrical strains in the L direction of the bar.

the orientations of the test pieces' axes with respect to the principal directions of the bar. The difference between the maximum and minimum diametral strains, i.e. the strain anisotropy, was greatest for test pieces parallel to the LT direction and least for those parallel to the ST direction. After ~0.9 true strain (150% elongation) the curves tend to become parallel, which indicates that the deformation was becoming less anisotropic. The curves also reveal that the strain anisotropy was independent of the initial strain rate in the superplastic deformation range. The surfaces of the longitudinal test pieces developed shallow grooves paralled to the rolling direction, whereas the long transverse and short transverse test pieces developed rumpled surfaces.

The effect of higher initial strain-rates in the nonsuperplastic range is shown in Figs. 5 to 7. The strain anisotropy increased in the L direction and showed no transition to isotropic flow, whereas the strain anisotropy decreased in the LT and ST directions. This difference in behaviour under superplastic and nonsuperplastic conditions is a consequence of different deformation processes occurring in these two states. This will be discussed later. Shear bands inclined at 45° to the tensile axis were visible on the surface of the longitudinal test piece after deformation at $\dot{\epsilon}_I = 1.05 \times 10^{-2}\,sec^{-1}$.

Deformation at 880° C and $\dot{\epsilon}_I = 4.2 \times 10^{-4}\,sec^{-1}$ was less superplastic than at 928° C and there was a tendency for multiple neck formation in the test pieces. The flow stresses in the L and LT directions were increased by a factor of 2 (to 25 MPa and 19 MPa, respectively), compared with values for the 928° C tests, but the respective strain anisotropies at 880 and 928° C were similar.

The transition from anisotropic to isotropic deformation indicated in Figs. 5 to 7 was examined in more detail by interrupting the superplastic deformation after predetermined strains. Data for these tests in the L and LT directions are compared with those for the continuous tests in Figs. 8 and 9. In the interrupted tests the maximum and minimum diameters were determined after increments of superplastic strain; after each increment

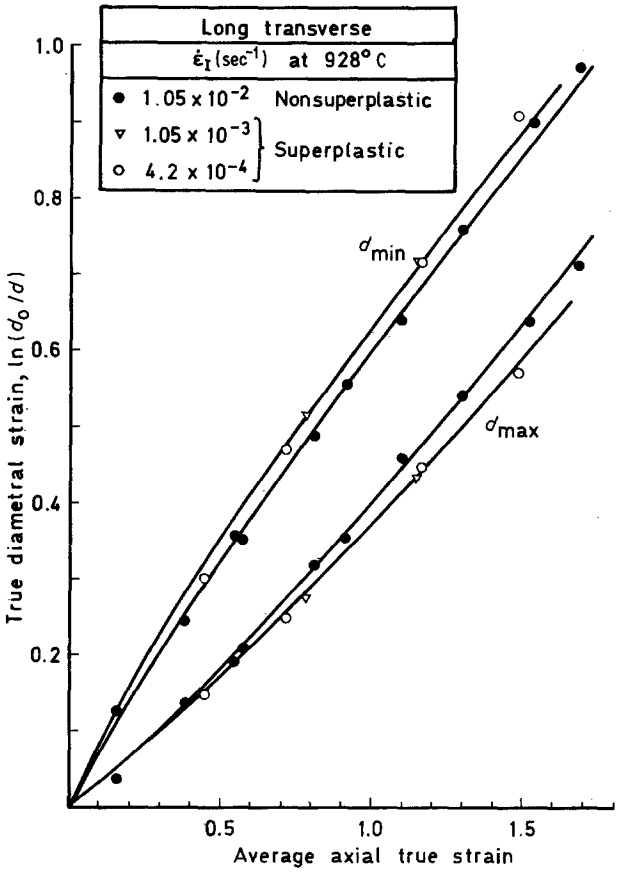

Figure 6 Effect of axial strain and strain rate on the maximum and minimum diametral strains in the LT direction of the bar.

the test piece was remachined and retested. The diameter ratios for the interrupted tests approached unity with increasing strain, i.e. the deformation became more isotropic after superplastic strain. For example, after a superplastic strain of 0.98, the diameter ratios for the L and LT test pieces were 0.845 and 0.76, respectively, after continuous tests but 0.97 and 0.95 after the interrupted tests. It was not possible to obtain comparable information on the effect of superplastic strain on flow stress from the present constant velocity tests, which involved some deformation in the test piece heads.

4. Discussion

The stress and strain anisotropy observed after elevated temperature superplastic deformation differed from that observed after room-temperature deformation. The room-temperature anisotropy was similar for mill annealed, heat cycled and superplastically deformed material and was related to the original crystallographic texture. This was not completely removed even after 1.48 superplastic strain (344%) at 928° C [21]. Typical room-temperature tensile properties and strain anisotropy, defined as d_{min}/d_{max}, are given in Table I. Evaluation of this data reveals that the highest flow stress is in the LT direction (parallel to the c-axis of the hcp lattice), whereas for superplastic deformation the highest flow stress is in the L direction (normal to the c-axis); see Fig. 2. The flow stresses in the three principal directions for room-temperature deformation are in the order $\sigma_{LT} > \sigma_L \geqslant \sigma_{ST}$ whereas for superplastic deformation the order is $\sigma_L > \sigma_{LT} > \sigma_{ST}$. The strain anisotropy data are compared in (the schematic diagram) Fig. 10, which shows the cross-sections after deformation in the three principal directions. The following observations may be made from this figure.

1. The cross-sections of test pieces orientated parallel to the c-axis (LT test pieces) were circular after deformation at room temperature (Figs. 10a and c) but were elliptical after superplastic deformation at 880° C and 928° C (Fig. 10b).

2. Elliptical cross-sections were obtained for

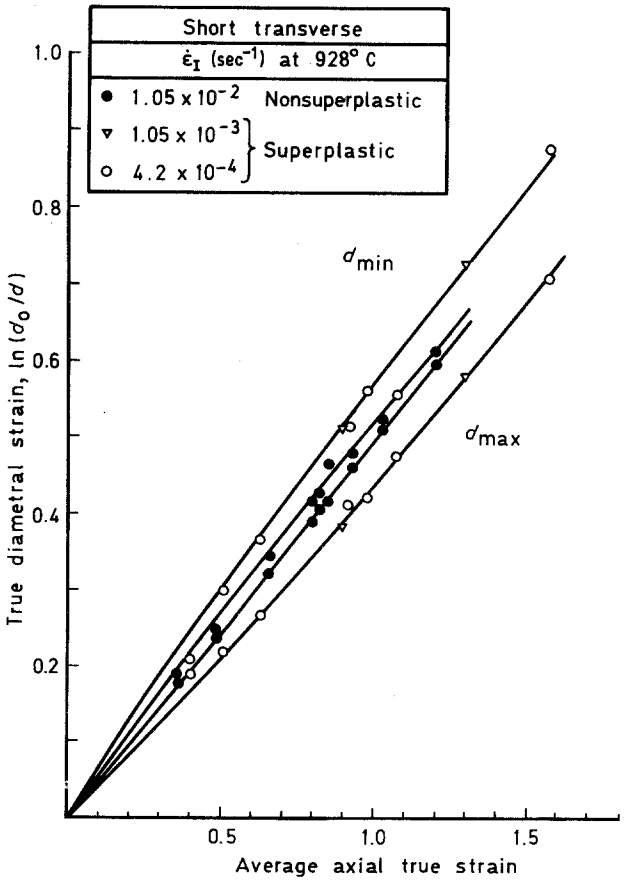

Figure 7 Effect of axial strain and strain rate on the maximum and minimum diametral strain in the ST direction of the bar.

test pieces orientated parallel to the ST direction after deformation at room temperature (Figs. 10a and c) and at the superplastic deformation temperature (Fig. 10b). However, the sense of the ellipticity, e.g. the direction of the maximum and minimum diametral strain, differed by 90° for these two conditions.

3. The cross-sections of the test pieces orientated parallel to the L direction were elliptical in the same sense after deformation at both room temperature (Figs. 10a and c) and at the superplastic temperature (Fig. 10b).

4. Superplastic strain did not affect room-temperature anisotropy of Figs. 10a and c.

TABLE I Effect of heat treatment and superplastic deformation on the room-temperature tensile properties of Ti–6 Al–4 V [21]

Condition		Property				
		0.2% PS (MPa)	TS (MPa)	E (GPa)	d_{min}/d_{max}	
					uniform	at fracture
Mill-annealed 4 h at 700° C AC	LT	987	1020	135	0.99	1.00
	L	897	942	115	0.96	0.85
	ST	895	945	114	0.98	0.84
Heat-cycled 0.5 h at 928° C FC	LT	973	1010	132	0.99	1.00
	L	875	916	116	0.96	0.82
	ST	849	910	110	0.99	0.82
Superplastically deformed ~ 150% at 928° C	LT	899	959	130	0.98	0.99
	L	874	920	118	0.97	0.84
	ST	878	915	118	0.98	0.89

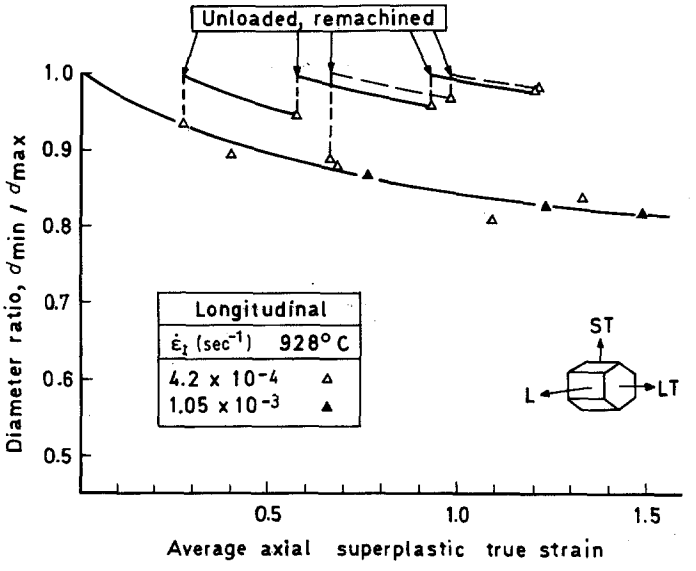

Figure 8 Effect of interrupted testing on the strain anisotropy in the L direction of the bar after superplastic deformation at 928° C.

It follows from point 4 that the room temperature deformation process of superplastically deformed material was controlled by the basal-edge texture which still remained after strains as high as 1.48 (344%). However, the results in Figs. 8 and 9 show that the superplastic deformation becomes more isotropic with increasing strain. Clearly, therefore, it must be the initial microstructure rather than the original crystallographic texture which controls the anisotropic superplastic deformation. The results also emphasise strongly the importance of making measurements in all the principal directions since information for the L direction alone would have been misleading. The present results therefore confirm the conclusion of Paton and Hamilton [17] that texture in the α-phase does not affect the ability of Ti–6 Al–4 V to deform superplastically and agrees with the observations of anisotropic superplastic deformation in eutectic Sn–Pb [6] and Al–Cu–Zr [11]. The transition from anisotropic to isotropic deformation is believed to be a consequence of grain-boundary sliding during the superplastic deformation progressively reducing the amount of aligned microstructure. Details of the microstructural and texture changes will be described in Part 2, based on [20]. The results for deformation at 880° C, which reveal that at this temperature the material was less superplastic and that the flow stresses were increased, did not sup-

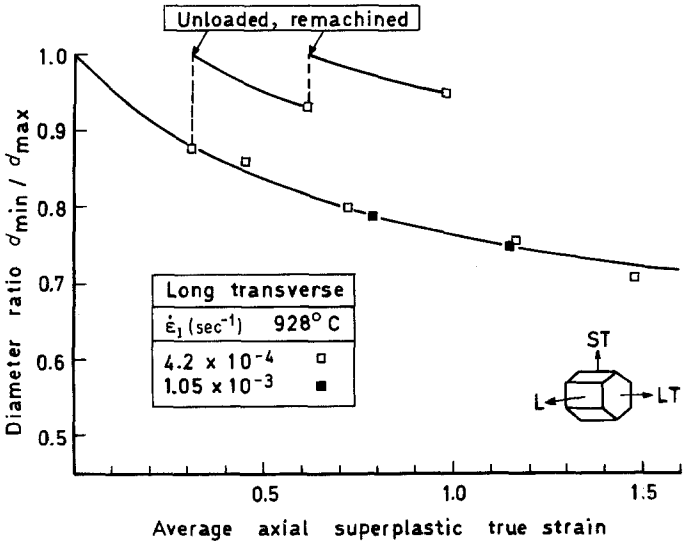

Figure 9 Effect of interrupted testing on the strain anisotropy in the LT direction of the bar after superplastic deformation at 928° C.

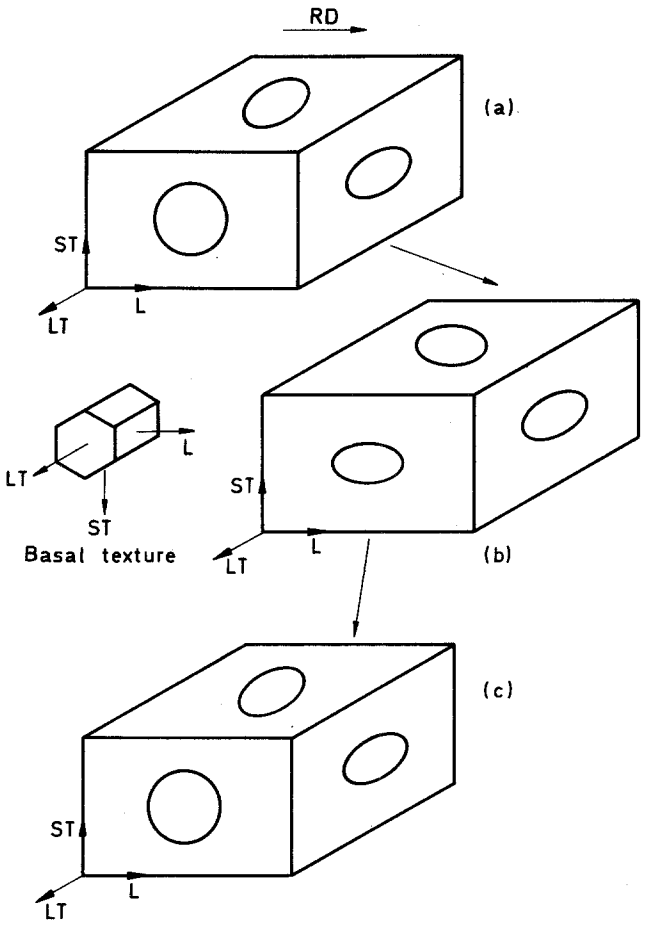

Figure 10 Schematic diagram of test piece cross-sections following uniaxial strain: (a) after room-temperature strain of mill-annealed material; (b) after superplastic strain at elevated temperature; and (c) after room-temperature strain following superplastic strain up to 344%.

port the observations of Kaibyshev *et al.* [19] that the presence of a strong texture reduces the superplastic forming stresses and permits the use of lower forming temperatures.

The role of texture in the elevated temperature deformation would be expected to increase with an increase in strain rate. In the present tests, under non-superplastic conditions the flow-stress anisotropy decreased with increasing strain-rate; see Fig. 2. At these strain rates the amount of grain-boundary sliding was significantly reduced, the microstructure remained aligned [20] and the critical resolved shear stresses for all the slip systems are likely to be similar. Unlike the strain anisotropy produced under superplastic conditions, the strain anisotropy under nonsuperplastic conditions (Figs. 5 to 7) was influenced by the original texture. For example the anisotropy was reduced in the LT direction, increased in the L direction and negligible in the ST direction. In the latter case the "apparent" isotropy appears to be a transition between ellipticity with the major axis parallel to the c-axis (Fig. 10a) and ellipticity with the major axis normal to the c-axis (Fig. 10b).

5. Conclusions

1. Stress and strain anisotropy was observed after superplastic deformation at 880 and 928° C in strongly textured Ti–6 Al–4 V bar. This anisotropy was a consequence of an aligned microstructure and was not dependent upon the crystallographic texture.

2. The superplastic deformation became less anistropic with increasing superplastic strain due to the progressive breakdown of the aligned microstructure by grain-boundary sliding.

3. Under non-superplastic forming conditions at high strain-rates the stress anisotropy decreased with increasing strain-rate whereas the strain anisotropy was influenced by both the aligned microstructure and the crystallographic texture.

Acknowledgements

This paper was published with the kind permission

of the Royal Aircraft Establishment, Farnborough.

References

1. J. W. EDINGTON, K. N. MELTON and C. P. CUTLER, *Progr. Mater. Sci.* **21** (1976) 61.
2. K. A. PADMANABHAN and G. J. DAVIES, "Superplasticity" – Materials Research and Engineering, Vol. 2 (Springer, Berlin, 1980).
3. C. M. PACKER, R. H. JOHNSON and O. D. SHERBY, *trans. AIME* **242** (1968) 2485.
4. R. H. JOHNSON, C. M. PACKER, L. ANDERSON and O. D. SHERBY, *Phil. Mag.* 18 (1968) 1309.
5. U. HEUBNER, K. N. MATUCHA and H. SANDIG, *Z. Metallkd.* **63** (1972) 607.
6. K. N. MELTON, C. P. CUTLER and J. W. EDINGTON, *Scripta Metall.* 9 (1975) 515.
7. D. M. R. TAPLIN *et al.* Proceedings of the 2nd International American Conference on Metals Technology, Vol. 1 (ASME, New York, 1970) p. 253.
8. G. L. DUNLOP, J. D. READ and D. M. R. TAPLIN, *Metall. Trans.* **2** (1971) 2308.
9. G. L. DUNLOP and D. M. R. TAPLIN, *J. Aust. Inst. Met.* **16** (1971) 195.
10. H. NAZIRI and R. PEARCE, *J. Inst. Met.* 98 (1970) 71.
11. R. H. BRICKNELL and J. W. EDINGTON, *Acta Metall.* **27** (1979) 1313.
12. D. LEE, *J. Inst. Met.* **99** (1971) 66.
13. F. LARSON and A. ZARKADES, "Properties of Textured Titanium Alloys", MCIC Rep.-74-20, June 1974.
14. A. W. BOWEN, *Mater. Sci. Eng.* **40** (1979) 31.
15. P. J. E. FORSYTH and C. A. STUBBINGTON, *Metals Tech.* **2** (1975) 158.
16. P. G. PARTRIDGE, *Met. Rev.* **118** (1968) 169.
17. N. E. PATON and C. H. HAMILTON, *Metall. Trans.* **10A** (1979) 241.
18. Y. LU, V. RAMACHANDRAN and R. E. REED-HILL, *ibid.* **1** (1970) 447.
19. O. A. KAIBYSHEV, I. V. KAZACHKOV and R. M. GALEEV, *J. Mater. Sci.* **16** (1981) 2501.
20. D. S. McDARMAID, A. W. BOWEN and P. G. PARTRIDGE, RAE Technical Report 83066 (1983).
21. *Idem, ibid.* 82108 (1982).

Received 7 October
and accepted 26 October 1983